Search for μ-e Conversion in Ti

D. A. Bryman, E. T. H. Clifford, M. J. Leitch,[a] I. Navon, T. Numao,[b] and P. Schlatter
TRIUMF and University of Victoria, Vancouver, British Columbia, Canada V6T 2A3

and

M. S. Dixit, C. K. Hargrove, and H. Mes
National Research Council of Canada, Ottawa, Ontario, Canada K1A 0R6

and

R. A. Burnham, M. Hasinoff, and J.-M. Poutissou
TRIUMF and University of British Columbia, Vancouver, British Columbia, Canada V6T 2A3

and

J. A. Macdonald and J. Spuller
TRIUMF, Vancouver, British Columbia, Canada V6T 2A3

and

G. Azuelos,[b] P. Depommier, J.-P. Martin, and R. Poutissou
Université de Montréal, Montréal, Québec, Canada H3C 3J7

and

M. Blecher and K. Gotow
Virginia Polytechnic Institute and State University, Blacksburg, Virginia 24061

and

A. L. Carter
Carleton University, Ottawa, Ontario, Canada K1S 5B6

and

H. L. Anderson
Los Alamos Scientific Laboratory, Los Alamos, New Mexico 87545

and

S. C. Wright
University of Chicago, Chicago, Illinois 60637

(Received 5 April 1985)

A search has been performed for the lepton-flavor-nonconserving reaction $\mu^- + \mathrm{Ti} \rightarrow e^- + \mathrm{Ti}$ using a time-projection chamber. No candidate events were observed, resulting in a limit of

$$\frac{\Gamma(\mu^- + \mathrm{Ti} \rightarrow e^- + \mathrm{Ti})}{\Gamma(\mu^- + \mathrm{Ti} \rightarrow \text{capture})} < 1.6 \times 10^{-11} \quad (90\%\ \text{C.L.})$$

for this reaction relative to ordinary muon capture.

PACS numbers: 13.60.–r, 11.30.–j, 14.60.–z, 25.30.Mr

Neutrinoless muon-electron conversion in the field of a nucleus

$$\mu^- + Z \rightarrow e^- + Z \qquad (1)$$

has been discussed as a potentially favorable process with which to search for lepton-flavor nonconservation.[1] Many attempts to incorporate multiple generations (flavors) into the standard model of weak interactions predict branching ratios for $\mu \rightarrow e$ conversion (1), $\mu \rightarrow e\gamma$, and $\mu \rightarrow 3e$ at the level of $< 10^{-9}$ relative to ordinary flavor-conserving processes, depending on the masses and couplings of hypothetical neutral particles which might mediate lepton-flavor–changing processes.[2–5] In some models,[5] mass limits in the multiteraelectronvolt range for new particles such as flavor-changing Higgs scalars and leptoquarks have been obtained from the experimental upper limits for these reactions. The signature of

coherent $\mu \rightarrow e$ conversion (1) in which the nucleus remains in the ground state is a single peak at the electron energy $E_e \sim m_\mu c^2 - B$, where m_μ and B are the muon mass and the binding energy of the muonic atom, respectively. The incoherent reaction leading to excited nuclear states is suppressed because of the Pauli blocking effect. Previous limits (90% C.L.) set on coherent $\mu \rightarrow e$ conversion are

$$\frac{\Gamma(\mu^- \mathrm{Cu} \rightarrow e^- \mathrm{Cu})}{\Gamma(\mu^- \mathrm{Cu} \rightarrow \text{capture})} \leq 1.6 \times 10^{-8} \quad (2)$$

(Ref. 6) and

$$\frac{\Gamma(\mu^- \mathrm{S} \rightarrow e^- \mathrm{S})}{\Gamma(\mu^- \mathrm{S} \rightarrow \text{capture})} \leq 7 \times 10^{-11} \quad (3)$$

(Ref. 7). In this Letter, a new upper limit for $\mu \rightarrow e$ conversion in titanium ($E_e \sim 104$ MeV) is reported.

The detection system is based on a hexagonal time-projection chamber (TPC) shown in Fig. 1. The titanium target is mounted on the TPC axis surrounded by inner trigger counters consisting of six plastic scintillators and a cylindrical wire chamber. The outer trigger counters consist of six planar wire chambers each sandwiched between two plastic scintillators. On the top and sides of the magnet are two layers of drift chambers for detection of cosmic-ray–initiated events.

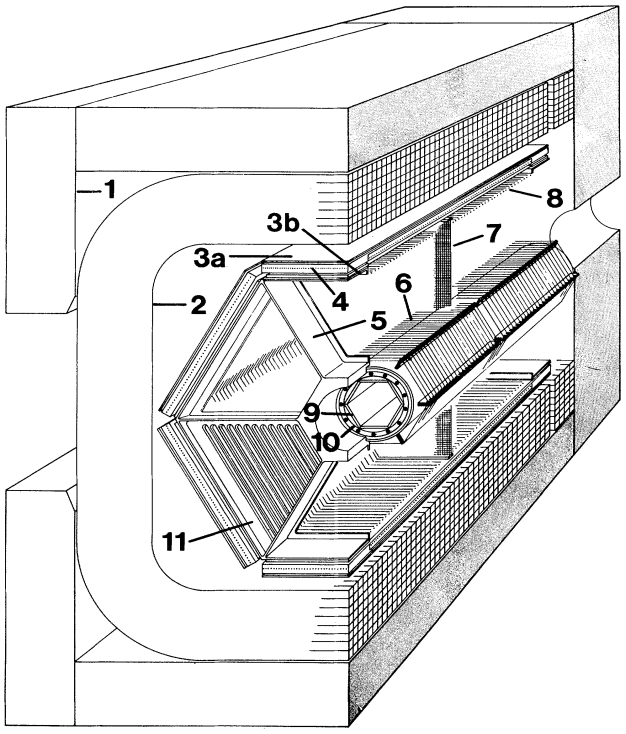

FIG. 1. A cut-away view of the TPC. The numbered elements are as follows: (1) the magnet iron, (2) the coil, (3a),(3b) outer trigger scintillators, (4) outer trigger proportional counters, (5) end-cap support frame, (6) inner electric field cage wires, (7) central high-voltage plane, (8) outer electric field cage wires, (9) inner trigger scintillators, (10) inner trigger cylindrical proportional wire chamber, and (11) end-cap proportional wire modules for track detection.

The TRIUMF TPC[8,9] is a large-volume atmospheric-pressure drift chamber situated in axially parallel magnetic and electric fields. Table I gives some of the TPC characteristics. Ionization electrons from a charged-particle track drift to the end caps of the chamber, where they are detected by a proportional wire system which gives independent x, y, and z coordinates. The position of each anode wire determines the y coordinate. The distribution of induced charges on the cathode, segmented into pads along the direction of the wire, is used to find the coordinate, x, along the anode wire. The drift time of the track segment to each wire gives the axial coordinate, z.

The apparatus was set up at the end of the M9 channel at TRIUMF. A 73-MeV/c μ^- beam was stopped at a typical rate of 5×10^5 s^{-1} in a 20-cm-long, shredded natural Ti target with a density of 0.1 g cm^{-3}. The raw μ^- beam contained a similar flux of pions and an order of magnitude more electrons. An rf particle separator[10] in the beam channel reduced the pion and electron contaminations to $\pi/\mu \approx 10^{-4}$ and $e/\mu \approx 10^{-2}$.

A stop signal opened a 600-ns-wide time gate during which an electron trigger, defined as a coincidence of both inner counter layers and at least two of the three outer layers, could be accepted. The trigger signal gated grids[9] on the appropriate TPC sectors, allowing ionization tracks to drift onto the end caps. Signals from ≥ 6 wires of the TPC were required in the event trigger. The magnetic field of 9 kG prevented most $\mu \rightarrow e\nu\bar{\nu}$ decay electrons from reaching the outer trigger counters. The typical event rate of 3 s^{-1} was due mostly to protons from μ^- capture reactions and low-energy electrons in coincidence with associated bremsstrahlung photons which fired the outer trigger detectors.

The data analysis was done in several steps. First,

TABLE I. TPC parameters.

Number of wires/sectors	144/12
Number of cathode pads per sector	636
Wire spacing	2.54 cm
Radial position of innermost wire	19.05 cm
Wire diameter	20 μm
Drift length	34.3 cm
Gas	Ar:CH_4(80:20), 1 atm
Drift velocity	7 cm/μs
Drift field	250 V/cm
Gas gain	5×10^4

the initial 2×10^7 events on tape were searched for tracks having ≥ 6 valid (x,y,z) points in the TPC and these were fitted to a helix. The momentum, energy loss, origin of the track, and other quantities were obtained from the fit and loose cuts were applied. The surviving data (approximately 10^6 events) were then subjected to more stringent cuts. Background events due to cosmic rays and beam pions were identified by the cosmic-ray veto counters and beam scintillators, respectively. A target-position cut was also effective in reducing these backgrounds. A χ^2 cut was used to remove events for which the track fit was unreliable.

The remaining $\mu \rightarrow e$ candidates and $\mu \rightarrow e\nu\bar{\nu}$ events above momentum $P = 80$ MeV/c, approximately 1000 events, were plotted for visual inspection. About 95% of the events passed this inspection. A momentum spectrum of those electron events with $P \geq 87$ MeV/c is shown by the solid-line histogram in Fig. 2. No candidate events were observed in the 97 to 105.5 MeV/c region. The expected number of events in this region due to cosmic rays and beam pions was estimated to be less than one.

The efficiency and resolution of the detector system were monitored at regular intervals in a stopping pion beam with use of the monoenergetic positrons (70 MeV/c) from the decay $\pi^+ \rightarrow e^+\nu$ under conditions similar to those in the $\mu \rightarrow e$ runs. For these tests, the magnetic field was lowered to 6 kG to reproduce the curvature of ~ 100-MeV/c $\mu \rightarrow e$ events at 9 kG. The acceptances measured in the $\pi \rightarrow e\nu$ runs included efficiency losses due to most cuts. Corrections for the other cuts, such as the target-position cut, were applied separately (because of the different stopping distributions of the pion and muon beams). A typical acceptance determined from the $\pi \rightarrow e\nu$ runs was $\sim 12\%$. Average correction factors applied to the acceptance as a result of the various cuts are listed in Table II.

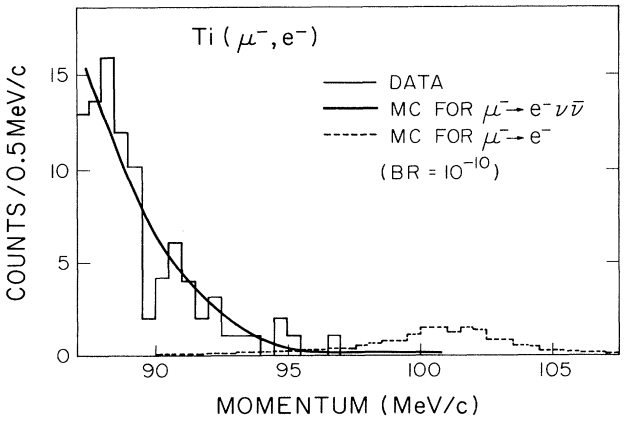

FIG. 2. Solid-line histogram: experimentally observed events. Solid curve: Monte Carlo simulation for $\mu^- \rightarrow e^-\nu\bar{\nu}$ decay in atomic orbit. Dashed-line histogram: Monte Carlo spectrum of $\mu^-\text{Ti} \rightarrow e^-\text{Ti}$ events for a branching ratio of 10^{-10}.

Correction for the momentum-window difference between the 67-MeV/c $\pi \rightarrow e\nu$ peak and the expected 101-MeV/c $\mu \rightarrow e$ peak (including a 3-MeV/c loss) was determined by Monte Carlo calculation. The calculation included the effect of $\mathbf{E}\times\mathbf{B}$ forces[8] on the track segments near the anode wires in the TPC, which results in a degradation of the resolution for positively charged particles compared to negatively charged ones. The calculated momentum resolution, found to be consistent with measurements, for the $\pi \rightarrow e\nu$ peak was 3 MeV/c (rms) whereas the expected resolution of the $\mu \rightarrow e$ conversion peak was 2 MeV/c (rms). The result of a Monte Carlo calculation corresponding to a branching ratio of 10^{-10} is shown by the dashed-line histogram in Fig. 2. The momentum window of 97 to 105.5 MeV/c for the observed spectrum would include 80% of all $\mu \rightarrow e$ conversion events.

The efficiency loss of 0.9 due to the π-background cut was deduced from the $\mu \rightarrow e$ runs by comparing the numbers of pion- and non-pion-associated events in the momentum region 60–70 MeV/c, where $\mu \rightarrow e\nu\bar{\nu}$ events are dominant. The correction for the 50–600-ns software time window on the muon capture lifetime in Ti was 0.7. The correction factor of 0.9 for the target-position cut was estimated from runs taken at a lower magnetic field to accept more $\mu \rightarrow e\nu\bar{\nu}$ decay events. The correction factor for the χ^2 cut and the visual inspection was estimated to be 0.9 from $\mu \rightarrow e\nu\bar{\nu}$ events in the 80–83-MeV/c region.

The average net efficiency over all running periods was $\bar{\Omega} \sim 4\%$. The number of muon stops in the Ti target was corrected for inefficiencies of the veto counters. This correction was deduced from the decay curve of $\mu \rightarrow e\nu\bar{\nu}$ events by fitting it with two decay components, $\tau_1 = 329.3$ ns for μ^- in titanium and $\tau_2 = 2026.3$ ns for μ^- in carbon.[11] A typical correction factor was 0.9.

Based on the absence of candidate events in 5×10^{12} stopped muons and the assumption of the Poisson dis-

TABLE II. Correction factors for the total acceptance.

$\pi \rightarrow e\nu$ acceptance		
(includes following cuts)		0.12
cosmic ray	0.8	
others	0.9	
χ^2 cut and visual inspection		0.9
Pion-background cut (beam)		0.9
Target-position cut		0.9
Time window		0.7
Energy window (97–105.5 MeV)		0.8

tribution, the upper limit for Reaction (1) is

$$R \equiv \frac{\Gamma(\mu^- + \mathrm{Ti} \rightarrow e^- + \mathrm{Ti})}{\Gamma(\mu^- + \mathrm{Ti} \rightarrow \mathrm{capture})} < \frac{2.3}{0.853 \sum_i N_i \Omega_i}, \quad (4)$$

$$R < 1.6 \times 10^{-11} \quad (90\%\ \mathrm{C.L.}), \quad (5)$$

where N_i is the number of stopped muons in Ti, Ω_i is the efficiency for a specific run period i, and 0.853 is the μ^--capture ratio in Ti. The confidence level does not include an estimated uncertainty of 20% in the efficiency. The solid line in Fig. 2 shows the result of Monte Carlo calculations for $\mu \rightarrow e\nu\bar{\nu}$ decay-in-orbit events corresponding to the present data. The spectrum was obtained with use of the calculations by Herzog and Alder[12] with $V-A$ couplings. The parametrization is valid within 20% for the region above 60 MeV/c. Good agreement between the calculation and the data was obtained. The contribution from radiative μ capture was less than 5% of the $\mu \rightarrow e\nu\bar{\nu}$ events and was neglected.

A branching ratio for incoherent processes was estimated to be $(0.0 \pm 2.0) \times 10^{-10}$ for the momentum region above 87 MeV/c by taking the difference between the experimental and the Monte Carlo $\mu \rightarrow e\nu\bar{\nu}$ spectra. The statistical error and the systematic errors in the normalization and in the Monte Carlo calculation were added quadratically. The dependence of the acceptance on momentum was obtained by Monte Carlo calculations.

The cutoff momentum of 87 MeV/c corresponds to an excitation energy $E_x = 14$ MeV of the residual nucleus. The photon spectrum from the reaction[13] $^{40}\mathrm{Ca}(\pi^-, \gamma)X$ was used to estimate the expected electron spectrum shape in the incoherent process for the momentum region below 87 MeV/c, since, kinematically, the incoherent $\mu \rightarrow e$ process is similar to the radiative capture of pions (π^-, γ) at rest. The fraction of the events below $E_x = 14$ MeV in the efficiency-corrected (π^-, γ) spectrum gave a multiplicative correction factor of 6.2. This led to an upper limit of 1.6×10^{-9} (90% C.L.) for the ratio of incoherent $\mu \rightarrow e$ conversion to the normal capture process.

According to Shanker,[14] for the vector-current case the coherent $\mu \rightarrow e$ conversion branching ratio can be expressed phenomenologically as the sum of isoscalar (g^0) and isovector (g^1) terms, arising from different couplings to up and down quarks. With use of the present upper limit (5) and the result of Ref. 7, the limit $|g^1| \leq 3.5 \times 10^{-5}$ is obtained, or alternatively, with the assumption of the same couplings for up and down quarks (i.e., $g^1 = 0$), $|g^0| \leq 2.5 \times 10^{-7}$.

We wish to thank P. Reeve, A. Otter, and L. P. Robertson for help in the early stages, the National Research Council physics workshop for the construction of the TPC, J. Cresswell, R. Skegg, and the TRIUMF electronics shop for designing and building the electronics for the trigger system and gating grids, L. Raffler and the Carleton University Science Technology Center and M. Salomon, C. Stevens, and the TRIUMF detector shop for construction of trigger counters, R. J. McKee, D. Kessler, W. Dey, D. Sample, S. Daviel, A. Bennett, C. Irwin, and W. R. Jack for software development, and J. Legault, J. Stapledon, R. Bula, and C. Lim for their technical help. This work was supported by the Natural Science and Engineering Research Council, the National Research Council of Canada, and the National Science Foundation.

[a]Present address: Los Alamos Scientific Laboratory, Los Alamos, New Mex. 87545.

[b]Present address: TRIUMF, 4004 Wesbrook Mall, Vancouver, British Columbia, Canada.

[1]G. Altarelli *et al.*, Nucl. Phys. **B125**, 285 (1977).

[2]T. P. Cheng and L. F. Li, Phys. Rev. D **16**, 1425 (1977).

[3]J. D. Bjorken and S. Weinberg, Phys. Rev. Lett. **38**, 622 (1977).

[4]W. J. Marciano and A. I. Sanda, Phys. Rev. Lett. **38**, 1512 (1977).

[5]O. Shanker, Nucl. Phys. **B206**, 253 (1982).

[6]D. A. Bryman *et al.*, Phys. Rev. Lett. **28**, 1469 (1972).

[7]A. Badertscher *et al.*, Nucl. Phys. **A377**, 406 (1982).

[8]C. K. Hargrove *et al.*, Nucl. Instrum. Methods **219**, 461 (1984).

[9]D. A. Bryman *et al.*, Nucl. Instrum. Methods **234**, 42 (1985).

[10]E. W. Blackmore *et al.*, Nucl. Instrum. Methods **234**, 235 (1985).

[11]T. Suzuki, Ph.D thesis, University of British Columbia, 1980 (unpublished).

[12]F. Herzog and K. Alder, Helv. Phys. Acta **53**, 53 (1980).

[13]J. A. Bistirlich *et al.*, Phys. Rev. C **5**, 1867 (1972).

[14]O. Shanker, Phys. Rev. D **20**, 1608 (1979).